

## Direct Observation of the Coexistence of the Pseudogap and Superconducting Quasiparticles in $\text{Bi}_2\text{Sr}_2\text{CaCu}_2\text{O}_{8+y}$ by Time-Resolved Optical Spectroscopy

Y. H. Liu,<sup>1,\*</sup> Y. Toda,<sup>2,3</sup> K. Shimatake,<sup>2,3</sup> N. Momono,<sup>4</sup> M. Oda,<sup>1</sup> and M. Ido<sup>1</sup>

<sup>1</sup>*Department of Physics, Hokkaido University, Sapporo 060-0810, Japan*

<sup>2</sup>*Department of Applied Physics, Hokkaido University, Sapporo 060-0810, Japan*

<sup>3</sup>*Division of Innovative Research CRIS, Hokkaido University, Sapporo 001-0021, Japan*

<sup>4</sup>*Department of Materials Science and Engineering, Muroran Institute of Technology, Muroran 050-8585, Japan*

(Received 8 February 2008; published 26 September 2008)

We report the ultrafast optical response of quasiparticles (QPs) in both the pseudogap (PG) and superconducting (SC) states of an underdoped  $\text{Bi}_2\text{Sr}_2\text{CaCu}_2\text{O}_{8+y}$  (Bi2212) single crystal measured with the time-resolved pump-probe technique. At a probe energy  $\hbar\omega_{\text{pr}} = 1.55$  eV, it is found that the reflectivity change  $\Delta R/R$  changes its sign at exactly  $T_c$ , which allows the direct separation of the charge dynamics of PG and SC QPs. Further systematic investigations indicate that the transient signals associated with PG and SC QPs depend on the probe beam energy and polarization. By tuning them below  $T_c$ , two distinct components can be detected simultaneously, providing evidence for the coexistence of PG and SC QPs.

DOI: [10.1103/PhysRevLett.101.137003](https://doi.org/10.1103/PhysRevLett.101.137003)

PACS numbers: 74.72.Hs, 68.37.Ef, 74.25.Gz, 74.50.+r

The relationship between the anomalous PG state and high- $T_c$  superconductivity is still an important open issue in condensed matter physics. To understand it well, two main scenarios have been put forward. One proposes that the PG state is dominated by a hidden order, which competes with high- $T_c$  superconductivity below  $T_c$  [1]. The other emphasizes that the PG state is a precursor of high- $T_c$  superconductivity [2]. In this picture, high- $T_c$  superconductivity originates from the PG state where Cooper pairs are formed but lack long-range phase coherence, which will be established below  $T_c$  [2]. Early angle-resolved photoemission spectroscopy (ARPES) and electron tunneling spectroscopy revealed that the PG could smoothly evolve into the SC gap as the temperature is lowered to below  $T_c$ , while electronic Raman scattering (ERS) data showed that nodal and antinodal gaps coexisted below  $T_c$  [3,4]. This discrepancy can be understood in terms of the scenario of the “Fermi-arc” superconductivity [4], which is supported by recent higher-resolution ERS [5] and ARPES [6–8] observations revealing that for underdoped cuprate superconductors, the SC gap located in the nodal region [4,6,9–11] is distinct from the PG located in the antinodal region, and these two gaps coexist below  $T_c$ .

Distinguishing the charge dynamics of QPs in the antinodal and nodal regions will be helpful as regards revealing the mechanism responsible for them. Time-resolved pump-probe optical spectroscopy with femto-second resolution is a powerful tool for determining the charge dynamics of carriers in superconductors [12]. In such measurements, a pump pulse with a higher energy than the SC energy gap breaks Cooper pairs into two electrons (or photoexcited carriers) and excites them to a nonequilibrium high-energy state. Subsequently, the probe pulse detects, within the delay time between the pump and probe pulses, the process

by which photoexcited carriers recombine into a superconducting condensate. Below  $T_c$ , the PG does not change into the SC gap for underdoped cuprate superconductors [3–8], meaning that the relaxation process of SC QPs (Cooper pairs) should differ from that of PG QPs. Therefore, in principle, this technique can be used to distinguish different relaxation processes involving PG and SC QPs in underdoped Bi2212 by measuring the sample reflectivity change  $\Delta R/R$ . Previously, pump-probe experiments revealed that  $\Delta R/R$  could be either positive or negative [13–18]. In particular, Mihailovic *et al.* [15,16,19,20] and Murakami *et al.* [17] have already conducted a self-consistent two-component analysis of the optical spectroscopy data obtained by the pump-probe technique, demonstrating that PG QPs coexist with SC QPs below  $T_c$ . However, a direct and unambiguous identification of distinct charge dynamics associated with SC and PG QPs still lacks. Recently, we have used two-color time-resolved pump-probe optical spectroscopy to investigate  $\text{NbSe}_3$  with two charge-density wave (CDW) transitions occurring at different temperatures [21], revealing that the two transitions can be selectively detected at temperatures far below the CDW transition temperatures. In this Letter, we report the direct identification of the charge dynamics of PG and SC QPs by measuring  $\Delta R/R$  of the underdoped Bi2212, using the same technique as that described in Ref. [21].

Underdoped Bi2212 single crystals with  $T_c = 76$  K (hole concentration 0.11) are grown by the traveling solvent floating zone method using an infrared image furnace. The time-resolved reflectivity change  $\Delta R/R$  is measured by using the pump-probe technique on the sample mounted in a cryostat whose temperature ranges from 4 to 300 K. Both the probe and pump beams are crossed and incident in

the  $c$ -axis direction on freshly cleaved surfaces. The laser power induced heating effect has been accounted for by measuring the temperature dependence of the  $\Delta R/R$  amplitude at different given powers. The pump-probe experimental configurations have been described in detail elsewhere [21]. It is worthwhile mentioning that the pump and probe fluences are  $\sim 40$  and  $\sim 10 \mu\text{J}/\text{cm}^2$ .

Figure 1(a) shows the temperature evolution of  $\Delta R/R$  as a function of delay time measured at a probe energy  $\hbar\omega_{\text{pr}} = 1.55 \text{ eV}$  and a pump energy  $\hbar\omega_{\text{pu}} = 1.07 \text{ eV}$  over a wide temperature range from 15 to 280 K. This waterfall plot shows that the sign changes of  $\Delta R/R$  occur just at the SC transition temperature  $T_c$  and the PG-opening temperature  $T^*$ , respectively. It should be pointed out that the  $T^*$  determined here is consistent with the result of the tunneling spectroscopy [22]. The sign of  $\Delta R/R$  below  $T_c$  and above  $T^*$  is positive, whereas it is negative between  $T_c$  and  $T^*$ . Hereafter, we define the positive (negative) signal as one with a positive (negative) sign. Using a single-component exponential decay function  $\Delta R/R(T, t) = A(T) \exp(-t/\tau)$ , where  $A(T)$  is the amplitude of  $\Delta R/R$  as a function of temperature ( $T$ ) and  $\tau$  is the relaxation time of QPs, we can fit the data well [solid lines in Figs. 1(b)–1(d)] and achieve the relaxation times for different QPs, whose temperature dependence is shown in Fig. 2(a). Considering the noticeable sign changes of  $\Delta R/R$  present at  $T_c$  and  $T^*$ , we naturally assign the positive component appearing below  $T_c$  with a slow decay of  $\sim 2.5 \text{ ps}$  to SC QPs (Cooper pairs), which corresponds to the recombination time of Cooper pairs, consistent with

those obtained on  $\text{Y}_{1-x}\text{Ca}_x\text{Ba}_2\text{Cu}_3\text{O}_{7-\delta}$  single crystal [16] and underdoped Bi2212 film [17] using two-component analysis. Another component that appears above  $T_c$  and fades out at  $T^*$  is ascribed to PG QPs with a relaxation time of  $\sim 0.5 \text{ ps}$ . The third component appearing above  $T^*$  is a step-function response with a relaxation time of  $\sim 0.8 \text{ ps}$  [Fig. 1(d)], which is a typically bolometric effect in the metal [23] and similar to that observed in  $\text{YBa}_2\text{Cu}_3\text{O}_{7-\delta}$  (Y123) at 300 K [24]. This observation is consistent with ARPES results showing that underdoped Bi2212 is a metal above  $T^*$  [25]. In this Letter, we focus our attention on the two components present below  $T^*$ . The temperature dependence of the amplitude of  $\Delta R/R$  is shown in Fig. 2(b), which exhibits two features: (1) the amplitude of the positive SC component decreases with increasing temperature and becomes zero at  $T_c$ ; (2) the negative PG component starts to appear at  $T_c$  and fades out around  $T^*$ . Comparing Figs. 2(a) and 2(b) carefully, one can find that at temperatures just above  $T_c$ , both the lifetime and amplitude of PG QPs are smaller than those well above  $T_c$  (around 90 K). If there is no superconductivity, it is speculated that the lifetime of PG QPs should be longer at lower temperatures because of lower scattering rates. This phenomenon seems to suggest that below  $T_c$  or around  $T_c$ , the PG state is slightly suppressed by high- $T_c$  superconductivity. This point will be discussed in the forthcoming paper in detail.

Figures 3(a) and 3(b) show the effect of the probe beam polarization on  $\Delta R/R$  measured at  $\hbar\omega_{\text{pr}} = 1.55 \text{ eV}$  below and above  $T_c$ . It is worthwhile noting that  $\Delta R/R$  shows no dependence on the pump beam polarization, which is consistent with previous reports on Y123 [20], but is closely related to that of the probe beam. Below  $T_c$ , the transient  $\Delta R/R$  is independent of the probe polarization, and two identical signals are obtained for  $\mathbf{E}_{\text{pr}} \parallel$  and  $\mathbf{E}_{\text{pr}} \perp$  ( $\mathbf{E}_{\text{pr}} \parallel$  and  $\mathbf{E}_{\text{pr}} \perp$  denoted as the probe polarizations parallel and orthogonal to the  $a$ -axis of the crystal, respectively).

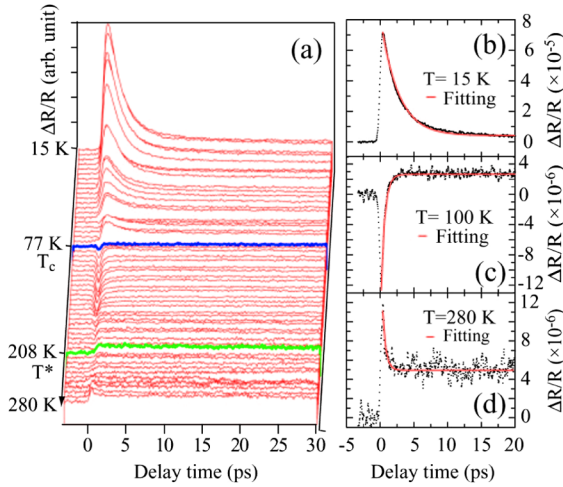


FIG. 1 (color online). (a) Waterfall plot for  $\Delta R/R$  as a function of delay time over a wide temperature range from 15 to 280 K measured at  $\hbar\omega_{\text{pu}} = 1.07 \text{ eV}$  and  $\hbar\omega_{\text{pr}} = 1.55 \text{ eV}$ . The pump and probe beams are polarized at  $90^\circ$  and  $0^\circ$  relative to the  $a$ -axis, respectively. The sign changes of  $\Delta R/R$  at  $T_c$  and  $T^*$  can be clearly seen. Note that the temperature of each curve corresponds to that of each point in Fig. 2. The single-component exponential function fittings are for transient signals measured at 15 K (b), 100 K (c), and 280 K (d).

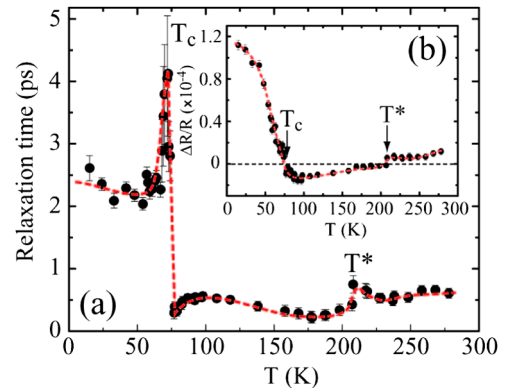


FIG. 2 (color online). Temperature dependence of (a) the relaxation time of QPs, and (b) the measured amplitude of  $\Delta R/R$  derived from the spectra shown in Fig. 1(a). The dashed lines are guides to the eye.

Above  $T_c$ , however, the  $\Delta R/R$  measured with  $\mathbf{E}_{pr} \perp$  is negative while that measured with  $\mathbf{E}_{pr} \parallel$  is negligible, which may be owing to the anisotropy of the probe transition matrix elements [26].

Further investigations indicate that the transient  $\Delta R/R$  also strongly depends on probe energy  $\hbar\omega_{pr}$ . In Figs. 3(c) and 3(d), the data measured after exchanging the pump and probe energies used above, i.e., measured at  $\hbar\omega_{pu} = 1.55$  eV and  $\hbar\omega_{pr} = 1.07$  eV, are shown. For  $\mathbf{E}_{pr} \perp$ , the sign of  $\Delta R/R$  measured at  $\hbar\omega_{pr} = 1.07$  eV is positive throughout the whole temperature range [Fig. 3(c)]. Above  $T_c$ , the one-component exponential decay function  $\Delta R/R(T, t) = A(T) \exp(-t/\tau_{PG})$  is used to fit the data well, resulting in the relaxation time  $\tau_{PG} \sim 0.5$  ps, which is equal to that measured at  $\hbar\omega_{pr} = 1.55$  eV in the PG state shown in Fig. 1(c). Since each kind of QP corresponds to one relaxation time, it is natural to assign this component to PG QPs. Below  $T_c$ , the signal consists of two components that have slow and fast decays, respectively. In this case, the analysis method is similar to that used in Refs. [16,17] and illustrated in the inset of Fig. 3(c). We first use a single-component decay function to fit the SC

and PG components, respectively, by fixing  $\tau_{PG} = 0.5$  ps and  $\tau_{SC} = 2.5$  ps and then obtain a sum of the above two fittings. It can be seen that this method works well, and we therefore assign the fast-decay component to PG QPs and the slow-decay component to SC QPs. For  $\mathbf{E}_{pr} \parallel$ , the detected signal consists of two distinct components with opposite signs below  $T_c$ , as seen in Fig. 3(d); the fast-decay component is positive and the slow-decay component is negative. A two-component decay function,  $\Delta R/R(T, t) = A(T) \exp(-t/\tau_{PG}) - B(T) \exp(-t/\tau_{SC})$ , is used to obtain a good fit with the data measured below  $T_c$ , using parameters of  $\tau_{PG} \sim 0.5$  ps and  $\tau_{SC} \sim 2.5$  ps. One fitting curve is shown as an example in the inset of Fig. 3(d). With increasing the temperature, the amplitude of the negative component decreases and becomes zero at  $T_c$ , suggesting that it originates from SC QPs. Above  $T_c$ , only the positive component remains whose relaxation time is about 0.5 ps, suggesting that the positive component observed below  $T_c$  is due to PG QPs. Therefore, we directly observe the coexistence of PG and SC QPs in underdoped Bi2212, which have different relaxation dynamics. This time-domain observation of the coexistence of PG and SC QPs below  $T_c$  is in good agreement with real-space measurements such as those obtained with scanning tunneling microscopy or spectroscopy (STM/STS) with atomic resolution, which reveal that SC and PG gaps coexist in real space in underdoped Bi2212 [10,11,27]. Here, we would like to emphasize that the coexistence of PG and SC QPs does not mean the ‘‘inhomogeneous phase separation’’ of the PG and SC states in real space. Recent STM/STS results suggest that both the PG and SC QPs should be distributed uniformly for a disorder-free underdoped Bi2212 sample below  $T_c$  [11,27,28].

In order to obtain detailed information on the energy dispersion of the charge dynamics of PG and SC QPs below  $T_c$ , we further investigate the effect of probe energy on the transient signal at 20 K, indicating that either the PG or SC component can be selectively detected at a specified probe energy. Figure 4(a) shows the signals measured at probe energies of 1.03 to 1.15 eV with  $\mathbf{E}_{pr} \parallel$ , which are normalized to the maximum absolute values of the amplitude of the negative component in the signals to minimize the effect of the pump power on the measured signal. As is clearly seen, two components originating with SC and PG QPs can be simultaneously detected, as discussed above. More interestingly, with increasing  $\hbar\omega_{pr}$ , the fraction of PG-component increases. At  $\hbar\omega_{pr} = 1.17$  eV, a single PG-component is detected [Fig. 4(b)]; i.e., the fraction of the PG component in the measured signal is almost 100%. As the probe energy increases further, the PG-component fraction decreases while the SC-component fraction increases; in the energy range from 1.39 to 1.77 eV only a single SC component is detected. To see this trend clearly, we show the amplitude ratio of the PG and SC components  $|\Delta R|_{PG}/|\Delta R|_{SC}$  equal to the values of  $A/B$ , which are

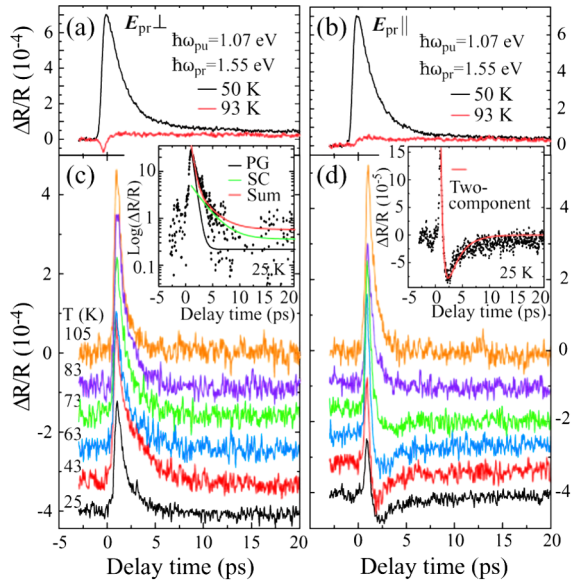


FIG. 3 (color online). The effect of probe polarization on the signal. The transient  $\Delta R/R$  measured at  $\hbar\omega_{pu} = 1.07$  eV and  $\hbar\omega_{pr} = 1.55$  eV both below and above  $T_c$  with (a)  $\mathbf{E}_{pr} \perp$  and (b)  $\mathbf{E}_{pr} \parallel$ . The transient  $\Delta R/R$  measured at  $\hbar\omega_{pu} = 1.55$  eV and  $\hbar\omega_{pr} = 1.07$  eV at various temperatures with (c)  $\mathbf{E}_{pr} \perp$  and (d)  $\mathbf{E}_{pr} \parallel$ . For clarity, each spectrum except for the topmost one is shifted by  $8 \times 10^{-5}$ . The inset in Fig. 3(c) shows the method used to analyze the signal measured at 25 K. The black line corresponds to single PG-component fitting, the gray line to single SC-component fitting, and the dashed line to the sum of the above two fittings. The inset in Fig. 3(d) shows the fitting using a two-component exponential decay function for the signal measured at 25 K (solid line).

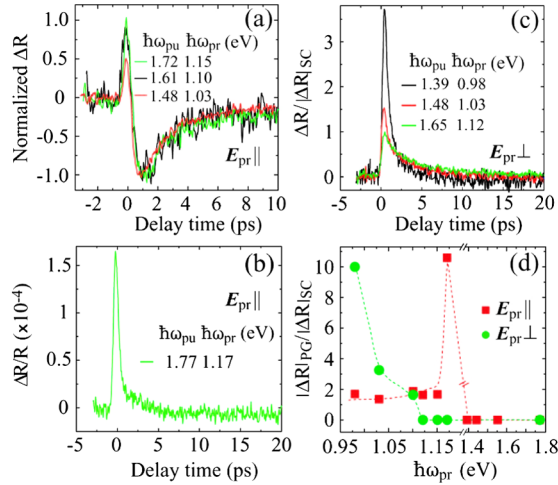


FIG. 4 (color online). The effect of probe energy on the signal measured at 20 K. (a) Normalized  $\Delta R$  measured at  $\hbar\omega_{pr}$  from 1.03 to 1.15 eV with  $\mathbf{E}_{pr}||$  by the maximum absolute value of the negative component. (b) Single PG component measured at  $\hbar\omega_{pr} = 1.17$  eV with  $\mathbf{E}_{pr}||$ . (c) Normalized  $\Delta R$  measured at  $\hbar\omega_{pr}$  from 0.98 to 1.12 eV with  $\mathbf{E}_{pr} \perp$ .  $|\Delta R|_{SC}$  is obtained from the single-component decay function by fixing  $\tau = 2.5$  ps. (d) Probe energy dependence of the amplitude ratio of the PG and SC components. This ratio is helpful in clarifying the change in the PG component with probe energy. The values of  $|\Delta R|_{PG}/|\Delta R|_{SC}$  are achieved from the fitting (see the details in the text).

obtained by fitting the signals using the function  $\Delta R/R(T, t) = A(T) \exp(-t/\tau_{PG}) - B(T) \exp(-t/\tau_{SC})$  [see the fitting method illustrated in the inset of Fig. 3(d)], as a function of  $\hbar\omega_{pr}$  for  $\mathbf{E}_{pr}||$  by solid squares in Fig. 4(d). These seem to surprisingly indicate that by tuning the probe energy, we can selectively detect different locations in the Fermi surface associated with PG and SC QPs.

The energy dependence of the signal measured with  $\mathbf{E}_{pr} \perp$  slightly differs from that measured with  $\mathbf{E}_{pr}||$ . For  $\mathbf{E}_{pr} \perp$ , the signal is always positive regardless of  $\hbar\omega_{pr}$ , as shown in Fig. 4(c). Careful fitting analysis indicates that at  $\hbar\omega_{pr} = 0.98$  eV the PG component dominates the signal. Increasing the probe energy results in a decrease in the PG component fraction and an increase in the SC component fraction; in the probe energy range from 1.12 to 1.77 eV, only the SC signal is detected. This trend is illustrated in Fig. 4(d) by solid circles, where the values of  $|\Delta R|_{PG}/|\Delta R|_{SC}$  are obtained by fitting the data using the method described in the inset of Fig. 3(c). Note that the signals measured at  $\hbar\omega_{pr} = 1.03$  and 1.10 eV are similar to those measured previously for La214 and Y123 samples [16,29] consisting of the mixed SC and PG components.

In summary, we unambiguously and directly distinguish the PG and SC QPs in the SC state below  $T_c$  with the time-resolved pump-probe optical spectroscopy by tuning the probe beam polarization and energy. The time-domain measurements reported here give strong support to the findings from ERS [3–5], ARPES [6–8], and STM/STS [10,11,27] that two kinds of QPs coexist below  $T_c$ .

This work was supported by the 21st century COE program “Topological Science and Technology” and Grants-in-Aid for Scientific Research from the Ministry of Education, Culture, Sports, Science and Technology, Japan.

\*Corresponding author: Present address: Department of Physics and Astronomy, Ohio University, Athens, OH 45701, USA; liuy@ohio.edu

- [1] For example, S. Chakravarty *et al.*, Phys. Rev. B **63**, 094503 (2001); V. Barzykin and D. Pines, Phys. Rev. B **52**, 13585 (1995); D. Pines, arXiv:cond-mat/0404151v1; C. M. Varma, Phys. Rev. Lett. **83**, 3538 (1999).
- [2] V. Emery and S. Kivelson, Nature (London) **374**, 434 (1995); Y. Yanase and K. Yamada, J. Phys. Soc. Jpn. **68**, 2999 (1999); S. S. Lee and S. -H. S. Salk, Phys. Rev. B **64**, 052501 (2001); M. Franz and Z. Tesanovic, Phys. Rev. Lett. **87**, 257003 (2001).
- [3] M. Opel *et al.*, Phys. Rev. B **61**, 9752 (2000).
- [4] M. Oda, N. Momono, and M. Ido, Supercond. Sci. Technol. **13**, R139 (2000), and references therein.
- [5] M. Le Tacon *et al.*, Nature Phys. **2**, 537 (2006).
- [6] K. Tanaka *et al.*, Science **314**, 1910 (2006).
- [7] T. Kondo *et al.*, Phys. Rev. Lett. **98**, 267004 (2007).
- [8] W. S. Lee *et al.*, Nature (London) **450**, 81 (2007).
- [9] M. Oda *et al.*, J. Phys. Soc. Jpn. **69**, 983 (2000).
- [10] K. McElroy *et al.*, Phys. Rev. Lett. **94**, 197005 (2005).
- [11] A. Hashimoto *et al.*, Phys. Rev. B **74**, 064508 (2006).
- [12] S. D. Brorson *et al.*, Phys. Rev. Lett. **64**, 2172 (1990).
- [13] S. G. Han *et al.*, Phys. Rev. Lett. **65**, 2708 (1990).
- [14] G. L. Eesley *et al.*, Phys. Rev. Lett. **65**, 3445 (1990).
- [15] V. V. Kabanov *et al.*, Phys. Rev. B **59**, 1497 (1999).
- [16] J. Demsar *et al.*, Phys. Rev. Lett. **82**, 4918 (1999).
- [17] H. Murakami *et al.*, Europhys. Lett. **60**, 288 (2002).
- [18] N. Gedik *et al.*, Phys. Rev. Lett. **95**, 117005 (2005).
- [19] T. N. Thomas *et al.*, Phys. Rev. B **53**, 12436 (1996).
- [20] C. J. Stevens *et al.*, Phys. Rev. Lett. **78**, 2212 (1997).
- [21] K. Shimatake, Y. Toda, and S. Tanda, Phys. Rev. B **75**, 115120 (2007).
- [22] R. M. Distasupil *et al.*, J. Phys. Soc. Jpn. **71**, 1535 (2002).
- [23] G. L. Easley, Phys. Rev. Lett. **51**, 2140 (1983).
- [24] W. Albrecht *et al.*, Phys. Rev. Lett. **69**, 1451 (1992).
- [25] M. R. Norman *et al.*, Nature (London) **392**, 157 (1998).
- [26] D. Dvorsek *et al.*, Phys. Rev. B **66**, 020510(R) (2002).
- [27] Y. H. Liu *et al.*, Phys. Rev. B **75**, 212507 (2007).
- [28] Y. H. Liu *et al.*, doi:10.1016/j.jpcs.2008.06.013.
- [29] S. Rast *et al.*, Phys. Rev. B **64**, 214505 (2001).